JEE Journal of Ecological Engineering

Journal of Ecological Engineering, 2026, 27(9), 366–380
https://doi.org/10.12911/22998993/222414
ISSN 2299–8993, License CC-BY 4.0

Received: 2026.05.12
Accepted: 2026.07.15
Published: 2026.08.01

Comparison of azo reactive and disperse dye decolorization via electro-oxidation and chemical coagulation

Pratin Kullavanijaya[1], Sirachon Arthasarnprasit[2], Supachai Hirunsupachote[3*], Orathai Chavalparit[2]

[1] Excellent Center of Waste Utilization and Management, Pilot Plant Development and Training Institute, King Mongkut's University of Technology Thonburi, Bangkok, 10150, Thailand
[2] Department of Environmental Engineering, Faculty of Engineering, Chulalongkorn University, Bangkok, 10330, Thailand
[3] Division of Environmental Science and Technology, Faculty of Science and Technology, Rajamangala University of Technology Phra Nakhon, Bangkok, 10800, Thailand
* Corresponding author's e-mail: supachai.h@rmutp.ac.th

ABSTRACT

The treatment of wastewater containing azo dyes, a primary textile industry effluent, is strongly governed by the dyes' chemical properties. Herein, the decolorization efficiency and operating costs of electro-oxidation (EO) using Pt/Ti electrodes and conventional chemical coagulation (CC) for treating synthetic wastewater containing either Azo Reactive Red 196 (ARR_{196}) or Azo Disperse Red 153 (ADR_{153}) were investigated. Operational parameters—including initial dye concentration ($C_{i,\,dye}$), applied current intensity (I_C), and wastewater feeding rate (F) for EO; and $C_{i,\,dye}$, aluminum sulfate dose (C_{Al}), and initial pH for CC—were optimized via the response surface methodology (RSM). The results indicate that dye structure and solubility significantly influence treatment efficiency and operating costs, as statistically confirmed via ANOVA for quadratic model predictions ($p < 0.05$ and R^2 values) for both EO and CC processes. Conventional CC was most effective for the low-solubility ADR_{153}, achieving a 97% removal efficiency at a low operating cost of 0.03 USD/m^3, compared to 57.5% at 0.15 USD/m^3 for ARR_{196}. In contrast, EO was superior for the highly soluble ARR_{196}, achieving an 83.3% decolorization efficiency at 0.024 USD/m^3, whereas ADR_{153} exhibited only 64.2% decolorization efficiency at a substantially higher operating cost of 1.63 USD/m^3. I_C and F were the critical factors ($p<0.05$) for the EO process, while pH was the primary determinant for CC. This study identified a direct correlation between specific chemical characteristics of pollutants and treatment efficiency, highlighting the necessity of selecting treatment technologies based on pollutant types to strategically optimize both economic and environmental outcomes.

Keywords: azo dye, chemical coagulation, electro-oxidation, process optimization, RSM.

INTRODUCTION

Colorant-bearing effluents from the textile and dyeing industry pose a significant threat to environmental sustainability. Throughout various production stages, the textile process generates finished products alongside hazardous pollutants in the forms of toxic gases, solid waste, and liquid effluents (Hassan and Carr, 2018). These effluents contain complex contaminants, including fibrous fragments, synthetic dyes, and trace metals, that are potentially harmful to both aquatic ecosystems and human health (Aquino et al., 2011; Ning et al., 2015). It is estimated that approximately 10% of global synthetic dye production is discharged annually through industrial waste streams (Sandhya et al., 2010). In addition, textile manufacturing is highly water-intensive, typically consuming between 200 and 400 liters per kilogram of product, primarily during washing and rinsing operations (Leal et al., 2019). Consequently, textile effluents exhibit intense coloration and high turbidity due to the presence of suspended solids, dyestuff, and oily scum (Kishor

et al. 2021). These characteristics significantly reduce sunlight penetration, inhibit aquatic photosynthesis, and disrupt oxygen transfer within waterbodies (Verma et al., 2012; Momeni et al., 2018). Furthermore, prolonged exposure to these chemical constituents may pose serious health risks, including hemorrhage, ulceration, skin irritation, nausea, and dermatitis (Elgarahy et al., 2021; Kyrii et al., 2020).

Currently, nearly 10,000 commercially produced dye types are available worldwide, with the annual global production of synthetic dyes and pigments at approximately 0.75 million tons. These colorants are extensively used for coloring fabrics and materials in the textile, cosmetics, and furnishing industries (Semeraro et al., 2015; Sharma, 2011). Synthetic dyes are generally classified into several categories, among which azo dyes represent the dominant group, accounting for 60–70% of total dye production (Zhou et al., 2019). Structurally, synthetic dyes consist of two principal components: chromophores, which impart color, and auxochromes, which facilitate dye fixation onto material surfaces. In azo dyes, the azo bond (-N=N-) serves as the primary chromophore, whereas the auxochromes groups determine whether the dye is classified as reactive, acidic, or disperse (Iqbal and Ashiq, 2008; Hunger, 2009). These functional groups strongly influence the dyes' applicability, solubility, and treatability characteristics (Andrade et al., 2007; Benkhaya et al., 2020). The utilization of azo dye varies according to fabric type. Approximately 0.18 million tons of azo reactive dyes are annually applied to cotton fibers (Hunger, 2009), whereas nearly 0.57 million tons of disperse dyes are used for synthetic materials such as polyester and nylon (Saritha et al., 2017). However, incomplete dyestuff fixation during textile processing results in substantial amounts of unfixed dyestuffs being discharged into wastewater, thereby causing major environmental threats.

Various physical, chemical, and biological processes have been developed for the treatment of dye-bearing wastewater (Robinson et al., 2001). Nevertheless, variations in production methods, fabric materials, and dye formations produce effluents with highly diverse characteristics, thereby influencing both treatment selection and decolorization efficiency. For instance, textile wastewater commonly exhibits low BOD/COD ratios, which limit the effectiveness of conventional biological treatment processes (Hao et al., 2000; Oller et al., 2011). Although carbon adsorption using activated carbon is highly effective for color removal, its application remains economically challenging due to adsorbent regeneration requirements and secondary waste management. Similarly, advanced oxidation processes (AOPs) efficiently degrade organic pollutants and refractory compounds; however, their efficiencies often decline in effluents containing high concentrations of dyeing auxiliaries and additives (Wang et al., 2020; Ferreira et al., 2020). Among the available alternatives, electrochemical technologies, particularly electro-oxidation (EO), have attracted increasing attention because of their high decolorization efficiency and potential flexibility (Donoso et al., 2021). In direct anodic oxidation, contaminants are oxidized directly on the anode surface, whereas indirect oxidation involves the electrochemical generation of oxidizing mediators, such as hypochlorous (HClO) and persulfate ($H_2S_2O_8$), which subsequently oxidize pollutants within the bulk solution. EO offers several advantages, including the efficient removal of toxic and non-biodegradable compounds without frequent electrode replacement or excessive sludge generation, thereby minimizing post-treatment disposal costs.

Despite the promising performance of EO for wastewater treatment (Brillas and Martinez-Huitle, 2015; Chou et al., 2011; Andrade et al., 2007; Rajkumar and Kim, 2006; Petrucci et al., 2015), conventional chemical coagulation (CC) remains one of the most widely applied technologies in textile wastewater treatment due to its economic feasibility and operational simplicity. CC is particularly effective for removing highly suspended solids and hydrophobic dyes. In this process, chemical coagulants, most commonly aluminum sulfate (alum), neutralizes the surface charges of dispersed dye particles, promoting the formation of charge-neutralized flocs that entrap organic matter and dyestuffs during precipitation. In contrast, indirect EO processes commonly employ chloride salt (e.g., NaCl) as supporting electrolytes to generate strong oxidizing chlorine species, including chlorine gas (Cl_2), hypochlorous acid (HClO), and hypochlorite ions (ClO^-). These oxidants subsequently diffuse into the wastewater and chemically degrade pollutants. Compared with direct oxidation alone, indirect EO generally achieves faster decolorization rates and provides more effective advanced oxidation pathways for pollutant degradation (Ahmed and Salman, 2023).

Nevertheless, the mechanisms underlying electrochemical degradation remain highly complex and strongly dependent on wastewater composition and operation conditions, thereby necessitating case-specific process optimization (Kasih, 2017). Traditional optimization approaches are often time-consuming and may fail to adequately capture the complex interactions among operational variables or account for partially understood reaction mechanisms. Moreover, limited information is available regarding how differences in dye chemistry influence treatment efficiency and process economic feasibility, particularly when comparing reactive and disperse azo dyes. Therefore, this study aimed to optimize the operating conditions and evaluate the interaction of key process variables on the treatment of synthetic azo dye-bearing wastewater using EO and CC processes (Khayet et al., 2011). Two representative azo dyes, azo reactive red 196 (ARR_{196}) and azo disperse red 153 (ADR_{153}), were selected and were compared in terms of decolorization performance and operating costs.

MATERIAL AND METHODS

Synthetic wastewater preparation

Two azo dyes with distinct solubilities and chemical structures—specifically Azo Reactive Red 196 (ARR_{196}) and Azo Disperse Red 153 (ADR_{153})—were selected for this study to represent high- and low-solubility groups, respectively (Figure 1). Individual synthetic wastewaters were prepared by dissolving each dye in tap water at three target concentrations (22, 25, and 28 mg/L) and adjusting the solution to the required pH using NaOH or H_2SO_4. This concentration range was selected based on the realistic median concentration of industrial textile effluent, which typically ranges from 10–50 mg/L, thereby ensuring the practical applicability of the optimized CC and EO processes via RSM. For the EO experiments, the wastewater conductivity was adjusted by adding two supporting electrolytes, sodium sulfate (Na_2SO_4) and sodium chloride (NaCl), each at 500 mg/L. This preparation protocol was applied consistently to both the EO and CC processes. The dye concentration of the initial and treated sample dye concentrations was quantified using the American Dye Manufacturers Institute (ADMI) color index to ensure standardized measurement and comparability across all experimental runs.

Electro-oxidation experimental set-up

EO experiments were performed in a rectangular acrylic reactor (dimensions: 50 × 5 × 8 cm) with an effective working volume of 2.0 liters, as illustrated in Figure 2. The electrode configuration consisted of three rectangular platinum-coated titanium (Pt/Ti) plates (dimensions: 400 × 50 × 1 mm) that functioning both anodes and cathodes in a symmetric electrode configuration. The inter-electrode distance was fixed at 5 mm to minimize Ohmic resistance and reduce electrical energy consumption, as smaller gaps are known to decrease the cell voltage required to maintain the target current intensity in textile effluent treatment. The efficiency of EO process is governed by the properties of electrode material; in this study, Pt/Ti was used as active anode. These electrodes pose a low oxygen evolution potential, which favors the chemisorption of radical leading to the partial oxidation of pollutants. Since NaCl was used as the supporting electrolyte, the 5 mm spacing facilitates the rapid transport of electrogenerated active chlorine species from the electrode surface into the bulk liquid, thereby enhancing the decolorization rate of the azo dyes. The reactor was operated under steady-state plug flow conditions. Electrical power was supplied to the

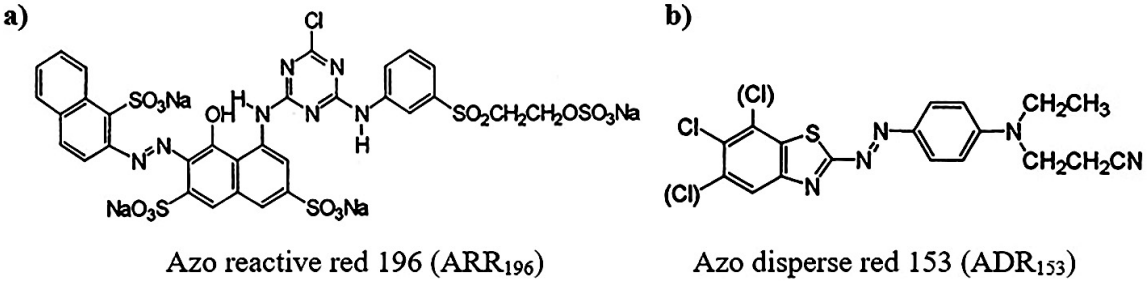

Figure 1. CI number and chemical structure of: (a) ARR_{196} and (b) ADR_{153}

electrodes via a DC power supply (GPR-606D) to maintain the prescribed levels of current and voltage. Following the wastewater feeding protocol, the colorant concentration was monitored periodically until a steady-state condition—defined herein as a stabilized pollutant removal rate—was achieved. The complete experimental assembly is shown in Figure 2.

Chemical coagulation-precipitation experimental set-up

CC experiments were conducted using a standard six-unit jar-test apparatus to facilitate the simultaneous evaluation of multiple operating conditions. For each run, 1.0 liter of synthetic wastewater was treated in a glass beaker using virgin alum (aluminum sulfate octadecahydrate, $Al_2(SO_4)_3.18H_2O$) as the primary coagulant. The experiment protocol followed a structured three-stage sequence of the standard treatment phases: initial rapid mixing at 250 rpm for 30 seconds to ensure homogeneous coagulant dispersion, follows by slow mixing for flocculation at 60 rpm for 30 minutes to destabilize and promote micro-floc aggregation or particle growth. Finally, the settling period, the sedimentation was performed by terminating the stirring, and the suspension was allowed to settle for 90 minutes. Following this period, the supernatant was collected for pH and residual color intensity analysis, with the latter quantified in ADMI units.

Process parameter optimization and analysis

The optimization of operating variables and their effects on the treatment efficiencies of the EO and CC processes were evaluated using response surface methodology (RSM) based on a three-level central composite design (CCD). This method is widely utilized for investigating the interactions of multiple factors within specific ranges. A full-factorial CCD with three coded levels (-1, 0, 1) was implemented for both processes, as summarized in Table 1. Each design variable was assigned a central coded value of zero. A second-order polynomial model was developed through multiple regression analysis to fit the experimental results of the CCD. The statistical significance of the interactions between process variables and responses was validated via analysis of variance (ANOVA). CCD is particularly suitable for such systems because it incorporates axial (star) points in addition to factorial and center points, enabling more accurate estimation of second-order polynomial models and response surface curvature. Both EO and CC experiments were conducted at ambient temperature ranging from 28–32 °C to reflect realistic operational conditions, which influence reaction rates and chemical solubility. Treatment performance was monitored by collecting effluent samples at specific time intervals until a steady-state condition was established. For the CC process, the initial pH value was adjusted according to the design specifications using 0.1 N HCl and 0.1 N NaOH. Both influent and effluent pH values were monitored using a pH meter. Color removal was determined by measuring absorbance at the maximum wavelength (λ_{max}) of 425 nm using a UV-visible spectrophotometer. The initial dye concentration was measured using a DR6000 UV-visible spectrophotometer equipped with RFID.

Color removal efficiency was calculated according to Equation (1):

$$Y_{COL} = \frac{C_{i,dye} - C_{f,dye}}{C_{i,dye}} \quad (1)$$

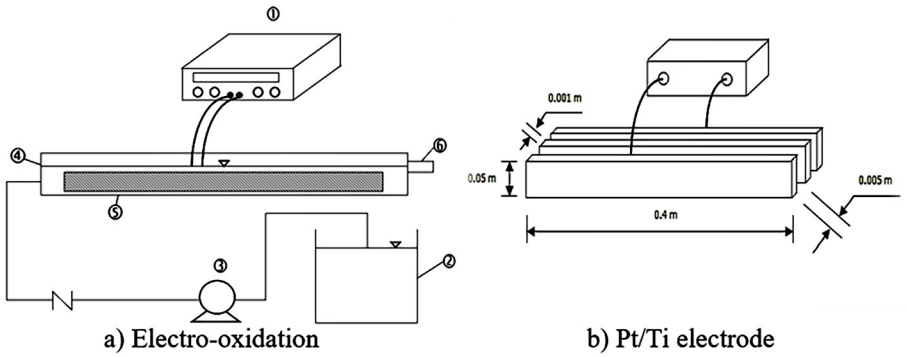

Figure 2. A set-up of an electro-oxidation chamber: (1) DC power supply; (2) wastewater feedstock; (3) influent feed pump; (4) electro-oxidation reactor; (5) Pt/Ti electrodes; (6) effluent line for the sample

Table 1. Symbol and coded factor of the three-level RSM designed for the selected azo dyes

Process	Factor	Unit	Symbol	ARR_{196}			ADR_{153}		
				Coded factor			Coded factor		
				-1	0	+1	-1	0	+1
Electro-oxidation	$C_{i,\ dye}$	mg/L	x_1	22	25	28	22	25	28
	I_C	A	x_2	0.7	1.0	1.3	2.4	3.0	3.6
	F	L/hr	x_3	12	15	18	1.8	2.4	3.0
Chemical coagulation	$C_{i,\ dye}$	mg/L	y_1	22	25	28	22	25	28
	pH	-	y_2	4.2	6	7.8	5.2	7	8.8
	C_{Al}	mg/L	y_3	250	400	550	100	115	130

where: $C_{i,\ dye}$ represents the initial dye concentration in the influent or feed wastewater, and $C_{f,\ dye}$ denotes the final color value.

The color intensity was determined in ADMI units, following APHA standard methods of 2120F (ADMI Weighted-Ordinate Spectrophotometer) and 2120E (ADMI Tristimulus Filter method).

Operational treatment cost estimation

Operational expenditure (OPEX) is a critical factor in determining the practical viability of various wastewater treatment technologies. This study evaluated and compared the operating costs of EO and conventional CC for treating synthetic azo dye wastewater. For EO, the primary operating cost is driven by electrical energy consumption, whereas the cost of the coagulant (aluminium sulfate or alum) is the dominant factor for coagulation. The optimization of color removal efficiency and associated operating costs was performed using the Design-Expert optimization module. The optimization was defined by two primary constraints: maximizing color removal and ensuring the final effluent concentration remained below the 300-ADMI-unit threshold. For the EO process, the operational parameters: $C_{i,\ dye}$, I_C, and F were maintained "within range" during the optimization procedure. Similarly, for the CC process, $C_{i,\ dye}$, C_{Al}, and pH were likewise kept "within range". The optimization of these parameters followed the objective functions defined in Equations (2) and (3).

$$\textit{Operational treatment cost of EO} = \left(\frac{baht}{kgdye}\right) = \frac{V \times I_C \times O}{F \times C_{i,dye} \times Y_{COL}} \quad (2)$$

The operating cost of the chemical coagulation process can be calculated by Equation 3.

$$\textit{Operational treatment cost of CC} = \frac{P \times C_{Al} \times 1L}{C_{i,dye} \times Y_{COL}} \quad (3)$$

In Equations 2 and 3, V is the applied voltage (volts). I_c is the applied current (amp). O is the electricity cost (0.086 USD/kWh). F is the wastewater feeding rate (L/h). $C_{i,\ dye}$ is the initial dye concentration (mg/L), and Y_{COL} is the color removal efficiency (%). Furthermore, P is the cost of alum (0.24 USD/kg alum), and C_{Al} is the alum concentration (mg/L).

Statistical analysis for mathematical equation prediction efficiency

The adequacy and prediction efficiency of the developed quadratic models were evaluated using Analysis of Variance (ANOVA). Key statistical indicators, including the coefficient of determination (R^2), adjusted R^2, and the Fisher's statistical test (F-test), were employed to determine the reliability of the mathematical equations in predicting the experimental responses. A p-value of less than 0.05 was considered statistically significant. The coefficient of determination (R^2) was used to evaluate the proportion of variability in the response that can be explained by the developed model. It was calculated by Equation (4):

$$R^2 = \frac{SS_{model}}{SS_{toal}} = 1 - \frac{SS_{residual}}{SS_{total}} \quad (4)$$

where: SS_{model}, SS_{model} and SS_{total} represent the model sum of squares, residual sum of squares, and total sum of squares, respectively.

To account for the number of model parameters and avoid overfitting, the adjusted coefficient of determination (R^2_{adj}) was calculated by (5)

$$R^2_{adj} = 1 - \left(\frac{SS_{residual}/df_{residual}}{SS_{tatal}/df_{total}}\right) \quad (5)$$

where: $df_{residual}$ and df_{total} are the degrees of freedom associated with the residual and total sum of squares, respectively.

The adjusted R^2 provides a more reliable measure of model performance, particularly for models with multiple predictors. The predictive capability of the model was evaluated using the predicted coefficient of determination (R^2_{pred}) which was calculated based on the Prediction Error Sum of Squares (PRESS) by Equation (6) and Equation (7):

$$R^2_{pred} = 1 - \frac{PRESS}{SS_{total}} \quad (6)$$

where: PRESS is defined as

$$PRESS = \sum\left(y_i - \hat{y}_{(i)}\right)^2 \quad (7)$$

where: y_i represents the experimental response and $\hat{y}_i$ is the predicted response obtained by excluding the *i*-th observation from the model fitting (leave-one-out cross-validation).

The adequacy and robustness of the developed models were evaluated based on the following criteria: High R^2 values indicating good model fit. Close agreement between R^2 and R^2_{adj}, suggesting minimal overfitting and a small difference between R^2_{adj} and R^2_{pred} (typically < 0.2), indicating good predictive capability.

RESULTS AND DISCUSSION

Statistically optimized process factor for azo dye treatment

RSM was employed to optimize the decolorization of azo dye wastewater and to evaluate the interactions among key operational parameters. The experimental results are detailed in Table 1, while the derived second-order polynomial regression models are provided in Equations (4–7). These mathematical expressions were utilized to construct three-dimensional (3D) response surface plots and to perform the ANOVA, as summarized in Table 2. For all developed models, a *p*-value < 0.05 indicated that the regression models were statistically significant at a 95% confidence level. Furthermore, the calculated F-values ranged from 8.78 to 21.64, which substantially exceeded the critical tabulated F-values ($F_{crit.}$) of 2.92 to 3.02. These high F-values, coupled with significant p-values, demonstrate that the models accurately represent the experimental space and the complex interactions between process variables.

EO process treatment efficiency:

For ARR_{196}:

$$R_1 = 71.77 - 2.17x_1 + 5.11x_2 - \\ - 7.24x_3 + 1.26x_1x_2 - 0.91x_1x_3 + 6.01x_2x_3 \quad (8)$$

$$Removal\ of\ ARR_{196}(\%) = 71.77 - \\ - 2.17C_{i,dye} + 5.11I_C - 7.24F + \\ + 1.26C_{i,dye}I_C - 0.91C_{i,dye}F + 6.01I_CF$$

For ADR_{153}:

$$R_2 = 35.77 - 0.31x_1 + 3.33x_2 - \\ - 9.92x_3 + 0.30x_1x_2 - 0.31x_1x_3 - \\ - 0.43x_2x_3 - 0.046x_1^2 + 0.66x_2^2 + 2.99x_3^2 \quad (9)$$

$$Removal\ of\ ADR_{153}(\%) = 35.77 - \\ - 0.31C_{i,dye} + 3.33I_C - 9.92F + \\ + 0.30C_{i,dye}I_C - 0.31C_{i,dye}F - \\ - 0.43I_CF - 0.046C_{i,dye}^2 + 0.66I_C^2 + 2.99F^2$$

where: R_1 is the color removal of reactive red 196, and R_2 is the color removal of ADR_{153}.

CC process treatment efficiency:

For ARR_{196}:

$$R_1^* = 45.46 + 1.65y_1 + 1.32y_2 + \\ + 18.42y_3 + 2.33y_1y_2 - 0.324y_1y_3 + \\ 0.198y_2y_3 - 2.01y_1^2 - \\ -3.87y_2^2 - 6.91y_3^2 \quad (10)$$

$$Color\ removal\ of\ ARR_{196}\ (\%) = 45.46 + \\ + 1.65C_{i,dye} + 1.32C_{Al} + 18.42pH + \\ + 2.33C_{i,dye}C_{Al} - 0.324C_{i,dye}pH + \\ 0.198C_{Al}pH - 2.01C_{i,dye}^2 - \\ - 3.87C_{Al}^2 - 6.91pH^2$$

For ARR_{156}:

$$R_2^* = 60.76 + 7.23y_1 + 9.93y_2 - \\ - 0.385y_3 - 7.83y_1y_2 + 7.85y_1y_3 + \\ 0.324y_2y_3 + 8.35y_1^2 + \\ + 6.90y_2^2 - 15.00y_3^2 \quad (11)$$

$$Color\ removal\ of\ ADR_{153}\ (\%) = 60.76 + \\ + 7.23C_{i,dye} + 9.93C_{Al} - 0.385pH - \\ - 7.83C_{i,dye}C_{Al} + 7.85C_{i,dye}pH + \\ 0.324C_{Al}pH + 8.35C_{i,dye}^2 + \\ + 6.90C_{Al}^2 - 15.00pH^2$$

where: R^*_1 is the color removal of ADR_{196} and R^*_2 is the color removal of ARR_{153}.

It is worth noting that a distinct divergence in model performance was observed between the EO and CC processes. The EO system exhibited higher F-values and greater consistency across all R^2 metrics, indicating a more deterministic and kinetically controlled regime. This behavior results in a relatively smooth response surface that is effectively captured by second-order polynomial models. A comparative evaluation using the coefficient of determination (R^2) confirmed the superior predictive performance of the electrochemical process, with EO models yielding higher R^2 values (0.908–0.943) compared to the CC models (0.837–0.888). These elevated values in the EO system are attributed to its relatively well-defined and reaction-controlled nature, governed primarily by direct electron transfer and indirect oxidation via hydroxyl radicals at the electrode surface. These mechanisms facilitate a predictable, continuous relationship between operating parameters—specifically I_c, F, and Ci, dye—and the decolorization response. Contrastingly, the CC process yielded lower R^2 values, particularly for ADR_{153} (R^2 = 0.837). This behavior reflects the inherently stochastic and multi-mechanistic nature of coagulation, which involves competing pathways such as charge neutralization, floc formation, particle aggregation, and sedimentation. These processes are highly sensitive to operating parameters such as pH and coagulant dosage; these parameters often exhibit non-linear transitions that are more difficult to approximate using quadratic models compared to the EO process. The comparative evaluation of mathematical predictions versus experimental performance for each dye is depicted in Figure 3.

Furthermore, a comparative analysis between ARR_{196} and ADR_{153} highlights the significant influence of molecular characteristics on model performance. While both dyes yielded high R^2 values in the EO process, the coagulation model for ADR_{153} demonstrated lower explanatory power. This suggests that complex interfacial phenomena, such as incomplete aggregation or the re-stabilization of colloidal particles, may be involved (Figure 1). Overall, the results indicate that EO is a more predictable and statistically robust process compared to CC. The superior R^2 values and enhanced model consistency suggest that EO is highly suitable for process modeling and optimization via RSM, whereas coagulation may require more advanced modeling approaches to fully capture its stochastic behavior. As summarized in Table 2, the statistical adequacy of the developed response surface

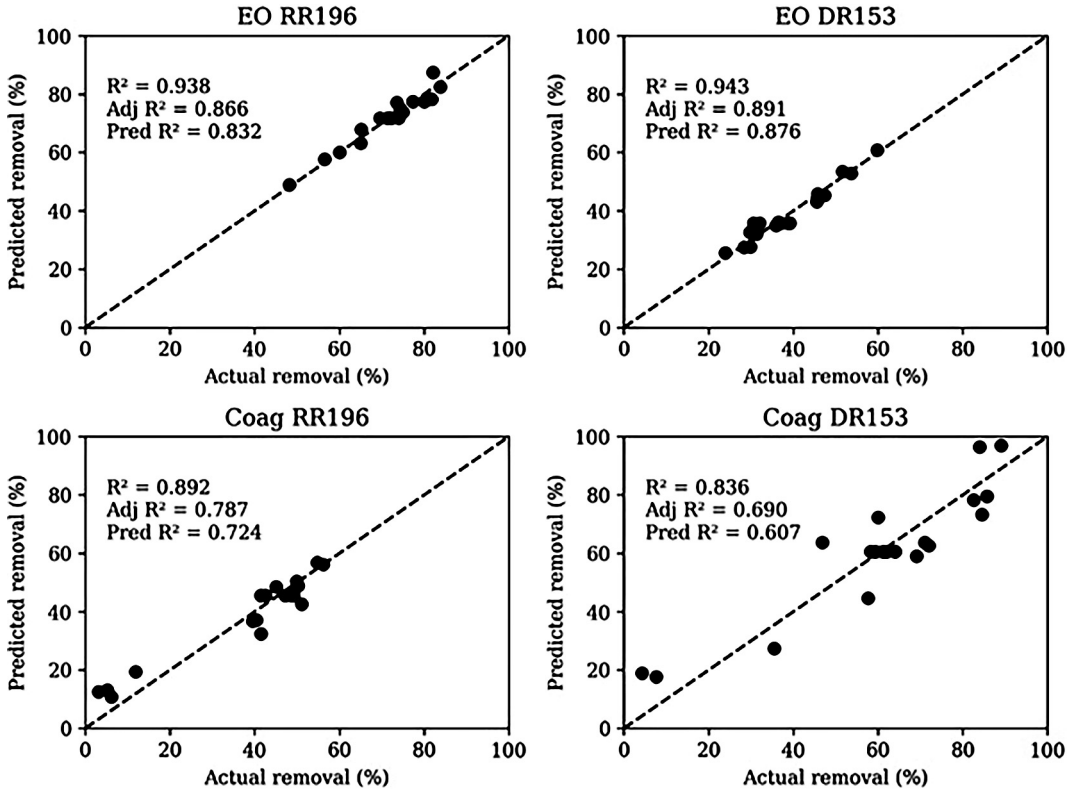

Figure 3. Comparative evaluation of mathematical prediction and experimental performance

models was evaluated using ANOVA in conjunction with goodness-of-fit and predictive performance indicators. All models were statistically significant (P<0.0001), with F-values ranging from 8.78 to 21.64, confirming that the selected operating variables and their interactions significantly influenced decolorization efficiency. The coefficient of determination (R^2) ranged from 0.837 to 0.943, demonstrating that the models explained a substantial proportion of experimental variability. Furthermore, the adjusted R^2 values (0.690–0.891) were in reasonable agreement with their corresponding R^2 values, indicating that the regression models were not overparameterized and that the included terms were statistically relevant. Finally, the predicted R^2 values (0.607–0.876) showed acceptable agreement with the adjusted R^2 values (|Adj R^2 − Pred R^2| < 0.2), confirming that the models possessed satisfactory predictive capability within the studied experimental domain.

Although the lack-of-fit was statistically significant ($p < 0.05$), the developed model was still considered acceptable for process optimization because the model exhibited high R^2, adjusted R^2, and predicted R^2 values with reasonable agreement among them. Furthermore, the model F-value was highly significant, indicating that the selected factors adequately described the experimental domain. The significant lack-of-fit may be attributed to the inherently complex and nonlinear behavior of the treatment system, particularly coagulation and interfacial interactions, which are difficult to fully capture using a second-order polynomial model.

EO process optimization via RSM for ARR_{196} and ADR_{153} decolorization

Herein, the effects of operational parameters—$C_{i,\ dye}$, I_C, and F—on decolorization performance of azo dye via EO process were investigated. The optimized results for the removal of ARR_{196} and ADR_{153} are illustrated in Figures 4 and 5. It was found that the I_C and F were the primary factors significantly affecting the decolorization of both dyes. An increase in I_C led to a substantial improvement in color removal ($p < 0.05$), attributed to the increased generation of oxidizing reagents with higher oxidizing potential. Conversely, by reducing F, the color removal efficiency was sharply increased. This increase is directly linked to an increase in the hydraulic retention time from 6 to 12 minutes, allowing for more contact between the pollutants and the electrode surface. This decolorization of the dye occurs through a dual mechanism: direct oxidation on the electrode surface and indirect oxidation mediated via the generation of the strong oxidants. Similarly, as reported by Szpyrokowicz et al. (2001), the electrolysis of NaCl and Na_2SO_4 generates powerful oxidizing agents that could facilitate this indirect process.

The addition of NaCl significantly enhanced the electro-oxidation performance by promoting the formation of active chlorine species, including hypochlorous acid (HOCl) and hypochlorite ions (OCl^-), which contributed to indirect oxidation pathways. At the anode surface, chloride ions were oxidized to chlorine gas, which subsequently hydrolyzed to form strong oxidizing agents capable of degrading azo dye molecules. These oxidants facilitated the cleavage of azo bonds (-N=N-) and oxidation of aromatic intermediates, thereby improving decolorization efficiency. The electrochemical reactions involved can be described as follows:

- Anodic chloride oxidation: $2Cl^- \rightarrow Cl_2 + 2e^-$
- Chlorine hydrolysis: $Cl_2 + H_2O \rightarrow HOCl + H^+ + Cl^-$
- Hypochlorite formation: $HOCl \leftrightarrow H^+ + OCl^-$

Table 2. ANOVA results for EO and CC treatments of ARR_{196} and ADR_{153}

Process	Source	ANOVA for ARR_{196}					ANOVA for ADR_{153}				
		DF	SS	MS	F-value	P-value	DF	SS	MS	F-value	P-value
EO	Model	6	1445	240.8	21.64	<0.0001	9	1632	240.8	18.21	<0.0001
	Residual	13	145.9	11.2	-	-	10	99.6	11.2	-	-
	Lack-of-fit	8	135.6	16.9	8.62	0.0165	5	35.2	16.9	0.75	0.7382
	Total	19	1591	-	-	-	19	1731	-	-	-
CC	Model	9	5589	74.54	8.78	<0.0001	9	8523	347.3	12.06	<0.0001
	Residual	10	707.3	2.64	-	-	10	1664	28.8	-	-
	Lack-of-fit	5	641.5	3.02	0.013	0.3798	5	1636	50.35	58.62	0.0002
	Total	19	6296	-	-	-	19	10187	-	-	-

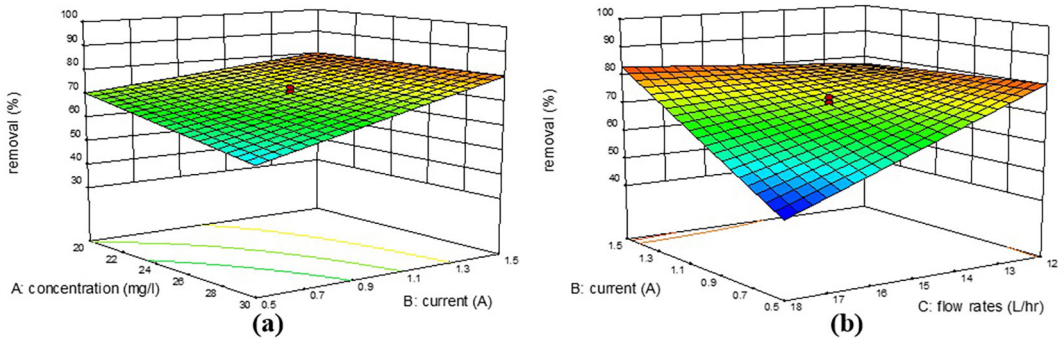

Figure 4. EO treatment efficiency for ARR_{196} at various conditions: (a) $C_{i,\,dye}$ vs I_C; (b) I_C vs F

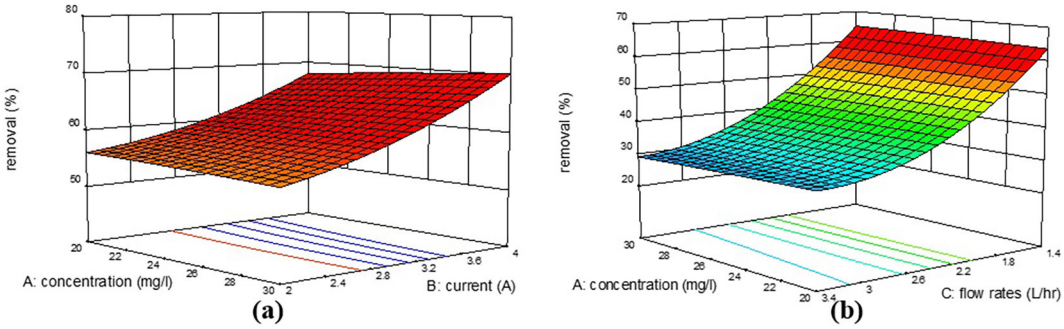

Figure 5. EO treatment efficiency for ADR_{153} at various conditions:(a) $C_{i,\,dye}$ vs I_C; (b) $C_{I,\,dye}$ vs F

- Azo bond degradation: R−N=N−R′+[O] → aromatic intermediates → CO_2+H_2O

These mechanisms are consistent with the experimental observations obtained in this study. Increasing the applied current intensity enhanced decolorization efficiency due to the greater generation of electrochemically active oxidants at the electrode surface. Conversely, lower flow rates improved treatment performance by increasing hydraulic retention time and promoting greater contact between oxidizing species and dye molecules. Furthermore, ARR_{196} exhibited superior electro-oxidation performance compared with ADR_{153}, which may be attributed to its higher aqueous solubility. The dissolved reactive dye molecules were more readily exposed to electro-generated oxidants, whereas the low solubility of ADR_{153} likely induced colloidal aggregation and mass-transfer limitations, thereby reducing oxidation efficiency and increasing energy consumption. Similar chloride-mediated indirect oxidation mechanisms have been widely reported in previous electrochemical treatment studies involving textile dye degradation.

In contrast, the initial dye concentration was found to have a negligible effect on decolorization efficiency within the studied range ($p > 0.05$). The optimal treatment condition, which promoted the maximum efficiency for ARR_{196} decolorization was achieved at a $C_{i,\,dye}$ of 28 mg/L, I_C of 1.06 A, and an F of 10 L/h, yielding 83.3% color removal. In comparison, the maximum decolorization for ADR_{153} was 64%, requiring a significantly higher I_C of 3.51 A, at an F of 10 L/h and a $C_{i,\,dye}$ of 23.3 mg/L. The requirement for a higher I_C and extended retention time for ADR_{153} is attributed to the low solubility of the dispersed azo dye, which imposes mass transfer limitations and consequently reduces the overall reaction rate. Finally, for the CC process, the initial pH was a critical factor; optimal decolorization was observed between pH 5 and 8, whereas highly alkaline conditions (pH >11) led to a reduction in removal efficiency due to the formation of soluble aluminate species and floc destabilization. The efficiency of the EO process in this study is highly sensitive to the initial pH, as the distribution of electro-generated active chlorine species is pH-dependent. When NaCl is used as the electrolyte, the anodic oxidation of chloride ions produces hypochlorous acid (HOCl) and hypochlorite ions (OCl-). Between

pH 3 and 7.5, HOCl is the predominant species. As HOCl is a significantly more powerful oxidant than OCl-, decolorization rates for ARR196 and ADR_{153} are typically enhanced in slightly acidic to neutral conditions. As the pH increases beyond 7.5, the equilibrium shifts toward the formation of OCl-, which has a lower oxidation potential (E^0 = 0.89V) compared to HOCl (E^0 = 1.49V), leading to the observed decrease in treatment efficiency at higher pH values. This speciation effect explains why the pH was identified by ANOVA as a significant factor influencing both the decolorization percentage and the overall operating costs.

CC process optimization via RSM for ARR_{196} and ADR_{153} decolorization

The optimization of operational parameters for the CC process, including $C_{i\,dye}$, C_{Al}, and pH in the removal of synthetic ARR_{196} and ADR_{153}, are illustrated in Figure 6 and 7. The results depicted that the decolorization of ARR_{196} by CC was strongly influenced by initial pH and C_{Al}, whereas the $C_{i,\,dye}$ exerted a negligible effect on the efficiency. Under the optimized conditions—a $C_{i,\,dye}$ of 24.9 mg/L, C_{Al} of 440.8 mg/L, and an initial pH of 8.75—a removal efficiency of ARR_{196} of approximately 57.5% was achieved. Color removal was minimal between pH 3 and 4, but increased sharply from pH 5 to 9. This change was attributed to the formation and precipitation of $Al(OH)_3(s)$ (Wong et al., 2007). This finding aligns with Yilmaz et al. (2007), who observed that the decolorization of Reactive Orange 16 via CC was closely related to pH, peaking within the neutral to alkaline range. Conversely, the critical parameters influencing ADR_{153} removal via CC were the $C_{i,\,dye}$ and pH. Due to its chemical structure and low solubility, the disperse dye is inherently more susceptible to adsorption and enmeshment within flocs than highly soluble reactive dyes. At the optimum conditions ($C_{i,\,dye}$ of 28.4 mg/L, C_{Al} of 136.7 mg/L, and pH of 7.59), a maximum decolorization of ADR_{153} of 97.2% was reached. Unlike the coagulation of ARR_{196}, the color removal efficiency increased proportionally with the $C_{i,\,dye}$, as depicted in Figure 7. Regarding pH, the color removal efficiency improved as the initial pH increased from 4.0 to 7.59, followed by a decline as the pH increased toward 10. This reduction at higher alkalinity is likely due to the formation of soluble aluminate ions, which leads to floc re-stabilization and a

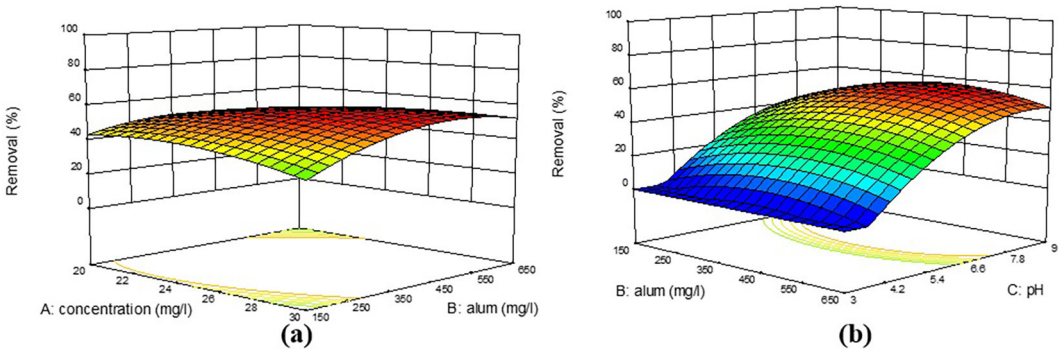

Figure 6. CC treatment efficiency for ARR_{196} at various conditions: (a) $C_{i,\,dye}$ vs C_{Al}; (b) C_{Al} vs pH

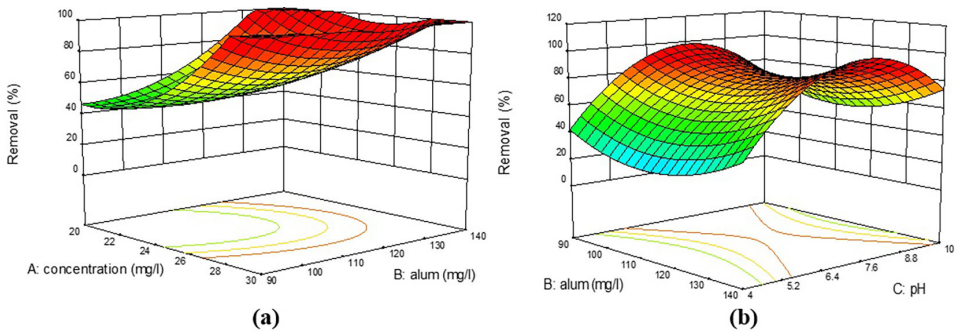

Figure 7. CC treatment efficiency for ADR_{153}: (a) $C_{i,\,dye}$ vs C_{Al}; (b) C_{Al} vs pH

decrease in the available surface area for adsorption (Kim et al., 2004).

In this study, the performance of chemical treatment processes was highly dependent on complex operational parameters, as precisely elucidated through RSM. The CCD model was applied with four factors and five levels, resulting in 30 experimental runs. A second-order polynomial was applied to correlate the responses with independent variables similar to Wong et al. (2007). Mechanistically, it was observed that dye degradation is highly governed by molecular structure. Azo dyes are electron-deficient molecules that typically undergo degradation via reductive cleavage of the azo linkage (-N=N-). The rate of decolorization is influenced by several intrinsic factors, including molecular weight, the presence of substituent groups, the number of azo bonds, and the formation of intermolecular hydrogen bonds between azo and hydroxyl groups (Johnstrup et al., 2011; Leal et al., 2019). Generally, azo dyes with simpler structures and low molecular weights exhibit higher rates of decolorization than those with high molecular weights and highly substituted molecules (Solis et al., 2012; De Oliveira et al., 2021). Furthermore, a direct correlation exists between hydraulic retention time (HRT) and color removal efficiency across various treatment pathways (Karatas et al., 2010; Da Silva et al., 2012; Spagni et al., 2010). For instance, extended HRT in anaerobic digestion enhances the activity of azo reductase enzymes responsible for bond cleavage and enhances color reduction (Johnstrup et al., 2011). In our EO and CC systems, sufficient contact time was similarly essential to facilitate either radical-mediated oxidation or floc-mediated adsorption. Conversely, high initial dye concentrations coupled with insufficient retention times significantly impeded removal efficiency, aligning with a previous study that found that dye concentration remains a critical factor, suggesting that lower concentrations (e.g., <50 mg/L) are most effectively decolorized.

Azo dye treatment cost via EO and CC processes

The optimization of process parameters for the treatment of ARR_{196} and ADR_{153} via EO and CC is summarized in Table 3. The operational expenditure (OPEX) and treatment efficiency varied significantly between the two methods, with both achieving a final concentration below the 300 ADMI threshold in specific cases. While the CC process successfully reduced the color of ADR_{153} to 69 ADMI units—well below the discharge threshold—the treatment of ARR_{196} via CC failed to meet the required wastewater standard. Economically, EO proved highly cost-effective for ARR_{196}, with an operating cost of only 0.024 USD/m^3. In contrast, the EO of ADR_{153} incurred a prohibitively high operating cost of 1.63 USD/m^3, rendering CC a more viable alternative for this specific dye. These findings align with previous research regarding the necessity of separate treatment streams for different dye classes, similar to the work of Wong et al. (2007), who found that the treatment efficiency of mixed azo reactive and disperse dyes varies significantly and depends heavily on the dye ratio and process synergy. Our results suggest that while mixed-dye treatment may offer operational simplicity, separate treatment allows for the optimization of specific mechanisms—oxidation for reactive dyes and coagulation for disperse dyes—thereby maximizing decolorization while minimizing OPEX. It is worth noting that the electrode stability and

Table 3. The operating cost comparison of the EO and CC processes at optimized conditions

Process	Optimized conditions	ARR_{196}	ADR_{153}
EO	Initial dye concentration (mg/L)	26.6	28.9
	Current (A)	0.51	2.26
	Flow rate (mg/L)	11.1	1.48
	Final concentration (ADMI)	256 (<300)	290 (<300)
	Operating cost (USD/m^3)	0.024	1.63
CC	Initial dye concentration (mg/L)	25	29.3
	Alum dosage (mg/L)	399.7	124.8
	Initial pH	7.84	7.59
	Final concentration (ADMI)	615 (>300)	69 (<300)
	Operating cost (USD/m^3)	0.15	0.03

durability were given less consideration due to the limitations of this laboratory-scale investigation. However, for practical applications, the operational lifetime of the catalytic coating is a critical consideration governing the long-term OPEX. This deterioration of the electrode is caused by several factors, such as the dissolution of the thin platinum layer or the growth of an insulating titanium dioxide layer (Moradi and Dehghanian, 2024). While the current study involved bench-scale experiments and confirmed short-term operational stability, further investigation is required to assess the true long-term stability and mechanical durability of the electrodes before integrating them into a continuous, industrial treatment plant.

While the EO process demonstrated high efficiency in decolourizing azo dyes by breaking down their parent chromophore structures, achieving complete oxidation is essential to ensure that no partially oxidised degradation products remain. Incomplete oxidation resulting from the cleavage of the -N=N- linkage occasionally yields intermediate compounds such as unsubstituted aromatic amines and benzene-ring derivatives, which are documented to possess toxic potential (Carrascal-Hernandez, 2025). To prevent the accumulation of these intermediates, the reaction must be driven toward complete mineralisation, converting these fragments thoroughly into CO_2 and H_2O. This complete oxidation can be achieved by optimizing operational process parameters, selecting suitable supporting matrices (Ridruejo et al., 2017) and integrating additional treatment processes, such as biological post-treatment.

Furthermore, the data gathered in this study demonstrated specific matching characteristics between the CC and EO processes, particularly for various azo dye types. This finding reveals distinct operational trade-offs regarding decolourization efficiency and operational costs for wastewater containing a single contamination source. The highly economical CC process is suitable for removing bulk colour and high organic loads, particularly when encountering low-solubility azo fractions. Conversely, EO exhibits superior capabilities for removing high solubilized recalcitrant structures, though at a higher energy penalty. Integrating both methodologies into sequential or hybrid processes represents a promising approach to achieving both high treatment efficiency and low operating costs in combined coloured wastewater treatment systems. However, this combination must be aligned with process selection criteria specifically related to the chemical properties of the dyes and the discharge standards required for the treated wastewater. Such integrated configurations can yield an overall synergistic performance that reduces pollutant concentrations, minimises chemical sludge management costs, and slashes electrochemical energy consumption compared to a standalone process (García-Montaño et al., 2015).

CONCLUSIONS

The results clearly demonstrate that molecular structure and aqueous solubility of azo dyes are the primary determinants of both treatment efficiency and operational cost. The high solubility of the azo dye ARR_{196} facilitated superior electro-oxidation (EO) performance, yielding high color removal efficiency at a negligible cost of 0.024 USD/m^3. In contrast, the EO treatment of the disperse dye ADR_{153} achieved only 64.2% removal efficiency, with a prohibitively high cost of 1.63 USD/m^3. This efficiency is attributed to the dye's slow solubility, which leads to the formation of recalcitrant colloids within the aqueous phase, thereby imposing mass-transfer limitations and consequently increasing energy consumption and operating costs. While the inlet flow rate (F) significantly influenced removal rates for both dyes, the data indicate a clear divergence in the optimal treatment method. ADR_{153} was effectively remediated via chemical coagulation (CC) at a minimal operational cost of 0.03 USD/m^3, whereas the CC of ARR_{196} failed to reduce the final concentration below the 300 ADMI threshold. These findings underscore the necessity of establishing selection criteria for azo dye wastewater treatment based on the specific chemical characteristics of the contaminants. Properties such as solubility, molecular weight, and ionic nature directly dictate both economic viability and treatment efficiency, suggesting that separate treatment streams are essential for optimizing industrial textile effluent management.

Acknowledgement

This work was financially supported by the 90th Anniversary of the Ratchadaphiseksomphot Endowment Fund of Chulalongkorn University (Grant No. 26.2015), the Office of the Higher Education Commission, and the Science and

Technology Postgraduate Education and Research Development Office. The authors gratefully acknowledge Rajamangala University of Technology Phra Nakhon for providing research facilities.

REFERENCES

1. Ahmed, Y.A., Salman, R.H. (2023). Simultaneous electrodeposition of multicomponent Mn–Co–Ni oxide electrodes for phenol removal by anodic oxidation. *Case Studies in Chemical and Environmental Engineering*, 8, 100386. https://doi.org/10.1016/j.cscee.2023.100386
2. Ali, S., Singh, R.P. 2009. Synthesis and characterisation of a modified chitosan. Macromol. *Symp*. 1e7. https://doi.org/10.1002/masy.200950301
3. Andrade, L. S., Ruotolo, L. A. M., Rocha-Filho, R. C., Bocchi, N., Biaggio, S. R., Iniesta, J., García-Garcia, V., Montiel, V. (2007). On the performance of Fe and Fe, F doped Ti–Pt/PbO_2 electrodes in the electro-oxidation of the Blue Reactive 19 dye in simulated textile wastewater.*Chemosphere*, 66(11), 2035-2043. https://doi.org/10.1016/j.chemosphere.2006.10.028
4. Andrade, L. S., Tasso, T. T., da Silva, D. L., Rocha-Filho, R. C., Bocchi, N., Biaggio, S. R. (2009). On the performances of lead dioxide and boron-doped diamond electrodes in the anodic oxidation of simulated wastewater containing the Reactive Orange 16 dye. *Electrochemica Acta*, *54*(7), 2024-2030. https://doi.org/10.1016/j.electacta.2008.08.026
5. Aquino, J. M., Pereira, G. F., Rocha-Filho, R. C., Bocchi, N, Biaggio, S. R. (2011). Electrochemical degradation of a real textile effluent using boron-doped diamond or β-PbO_2 as anode. *J Hazard Mater*, *192*(3), 1275–1282. https://doi.org/10.1016/j.jhazmat.2011.06.039
6. Asaithambi, P., Matheswaran, M. (2011). Electrochemical treatment of simulated sugar industrial effluent: Optimization and modelling using a response surface methodology. *Arabian Journal of Chemistry*. https://doi.org/10.1016/j.arabjc. 2011.10.004
7. Benkhaya, S., M'rabet, S., El Harfi, A. (2020). A review on classifications, recent synthesis and applications of textile dyes. *Inorganic Chemistry Communications*, *115*(2020), 107891. https://doi.org/10.1016/j.inoche.2020.107891
8. Brillas, E., Martínez-Huitle, C. A. (2015). Decontamination of wastewaters containing synthetic organic dyes by electrochemical methods. An updated review. *Applied Catalysis B: Environmental*, *166*, 603–643. https://doi.org/10.1016/j.apcatb.2014.11.016
9. Carrascal-Hernández, D. C., Orozco-Beltrán, E. J., Insuasty, D., Márquez, E., Grande-Tovar, C. D. 2025. Systematic evaluation of biodegradation of azo dyes by microorganisms: Efficient species, physicochemical factors, and enzymatic systems. International Journal of Molecular Sciences, 26(16), 7973. https://doi.org/10.3390/ijms26167973
10. Chou, W.-L., Wang, C.-T., Chang, C.-P. (2011). Comparison of removal of Acid Orange 7 by electro-oxidation using various anode materials. *Desalination*, *266*(1), 201–207. https://doi.org/10.1016/j.desal.2010.08.027
11. De Oliveira, C. R. S., da Silva Júnior, A. H., Mulinari, J., Immich, A. P. S. (2021). Textile Re-Engineering: Eco-responsible solutions for a more sustainable industry. *Sustainable Production and Consumption*, *28*(2021), 1232–1248. https://doi.org/10.1016/j.spc.2021.08.001
12. Donoso, G., Dominguez, J. R., González, T., Correia, S., Cuerda-Correa, E. M. (2021). Electrochemical and sonochemical advanced oxidation processes applied to tartrazine removal. Influence of operational conditions and aqueous matrix. *Environmental Research*, *202*(2021), 111517. https://doi.org/10.1016/j.envres.2021.111517
13. Elgarahy, A. M., Elwakeel, K. Z., Mohammad, S. H., Elshoubaky, G. A. (2021). A critical review of biosorption of dyes, heavy metals and metalloids from wastewater as an efficient and green process. *Cleaner Engineering and Technology*, *4*(2021), 100209. https://doi.org/10.1016/j.clet.2021.100209
14. Ferreira, L. C., Salmerón, I., Peres, J. A., Tavares, P. B., Lucas, M. S., Malato, S. (2020). Advanced Oxidation Processes as sustainable technologies to reduce elderberry agro-industrial water impact. *Water Resources and Industry*, *24*(2020), 100137. https://doi.org/10.1016/j.wri.2020.100137
15. Hao, O.J., Kim, H. and Chiang, P. (2000). Decolorization of wastewater. *Critical Reviews in Environmental Science and Technology*, *30*, 449–505. https://doi.org/10.1080/10643380091184237
16. Hassan, M. M., Carr, C. M. (2018). A critical review on recent advancements of the removal of reactive dyes from dyehouse effluent by ion-exchange adsorbents. *Chemosphere*, *209*(1), 201–219. https://doi.org/10.1016/j.chemosphere.2018.06.043
17. Hunger, K. (2009). *Industrial dyes: Chemistry, properties, applications*. Wiley-VCH. https://doi.org/10.1002/9783527623353
18. Iqbal, M. J., Ashiq, M. N. (2008). Adsorption of dyes from aqueous solutions on activated charcoal. *Journal of Hazardous Materials*, *139*(1), 57–66. https://doi.org/10.1016/j.jhazmat.2006.06.007
19. Jasim, R.A., Salman, R.H. (2024). Congo red removal from aqueous solution by electrocoagulation–electro-oxidation combined system with Al and Cu–Mn–Ni nano composite as efficient electrodes. *Case Studies in Chemical and Environmental*

Engineering, *9*, 100747. https://doi.org/10.1016/j.cscee.2024.100747

20. Johnstrup, M., Kumar, N., Murto, M., Mattiasson, B. (2011). Sequential anaerobic–aerobic treatment of azo dyes: Decolourisation and amine degradability. *Desalination*, *280*, 339–346. https://doi.org/10.1016/j.desal.2011.07.022
21. Kasih, T. P. (2017). Investigation of the non-thermal plasma-based advanced oxidation process to remove organic contaminants in the azo dye solution. *Journal of Ecological Engineering*, *18*(2), 1–6. https://doi.org/10.12911/22998993/68305
22. Khayet, M., Zahrim, A. Y., Hilal, N. (2011). Modelling and optimisation of coagulation of highly concentrated industrial grade leather dye by response surface methodology. *Chemical Engineering Journal*, *167*(1), 77–83. https://doi.org/10.1016/j.cej.2010.11.108
23. Kim, T.-H., Park, C., Yang, J., Kim, S. (2004). Comparison of disperse and reactive dye removals by chemical coagulation and Fenton oxidation. *J Hazard Mater*, *112*(1–2), 95–103. https://doi.org/10.1016/j.jhazmat.2004.04.008
24. Kishor, R., Purchase, D., Saratale, G.D., Saratale, R.G., Ferreira, L.F.R., Bilal, M., Iqbal, H.M.N. and Bharagava, R.N. (2021). Ecotoxicological and health concerns of persistent coloring pollutants of textile industry wastewater and treatment approaches for environmental safety. *Journal of Environmental Chemical Engineering*. *8*(6), 104504. https://doi.org/10.1016/j.jece.2020.104504
25. Kyrii, S., Dontsova, T., Kosogina, I., Astrelin, I., Klymenko, N., Nechyporuk, D. (2020). Local wastewater treatment by effective coagulants based on wastes. *Journal of Ecological Engineering*, *21*(5), 34–41. https://doi.org/10.12911/22998993/122184
26. Leal Filho, W., Ellams, D., Han, S., Tyler, D., Boiten, V., Paço, A., Moora, H. and Balogun, A.L. (2019). A review of the socio-economic advantages of textile recycling. *Journal of Cleaner Production*, *218*, 10–20. https://doi.org/10.1016/j.jclepro.2019.01.210
27. Merzouk, B., Gourich, B., Madani, K., Vial, C., Sekki, A. (2011). Removal of a disperse red dye from synthetic wastewater by chemical coagulation and continuous electrocoagulation. A comparative study. *Desalination, 272*(1–3), 246–253. https://doi.org/10.1016/j.desal.2011.01.029
28. Momeni, M.M., Kahforoushan, D., Abbasi, F., Ghanbarian, S. (2018). Using chitosan/CHPATC as a coagulant to remove colour and turbidity of industrial wastewater: optimisation through RSM design. *Journal of Environmental Management*, *211*, 347–355. https://doi.org/10.1016/j.jenvman.2018.01.031
29. Moradi, F., Dehghanian, C. (2014). Addition of IrO_2 to RuO_2–TiO_2 coated anodes and its effect on electrochemical performance of anodes in acid media. *Progress in Natural Science: Materials International, 24*(2), 134–141. https://doi.org/10.1016/j.pnsc.2014.03.002.
30. Ning, X. A., Wang, J. Y., Li, R. J., Wen, W. B., Chen, C. M., Wang, Y. J., Yang, Z. Y., Liu, J. Y. 2015 Fate of volatile aromatic hydrocarbons in the wastewater from six textile dyeing wastewater treatment plants. *Chemosphere*, *136*, 50–55. https://doi.org/10.1016/j.chemosphere.2015.03.086
31. Oller, I., Malato, S., Sánchez-Pérez, J.A. (2011). Combination of advanced oxidation processes and biological treatments f or wastewater decontamination-a review*, Science of the Total Environment*, *409*, *20*, 4141–4166. https://doi.org/10.1016/j.scitotenv.2010.08.061
32. Petrucci, E., Di Palma, L., Lavecchia, R., Zuorro, A. (2015). Treatment of diazo dye Reactive Green 19 by anodic oxidation on a boron-doped diamond electrode. *Journal of Industrial and Engineering Chemistry*, *26*, 116–121. https://doi.org/10.1016/j.jiec.2014.11.022
33. Rajkumar, D., Kim, J. G. (2006). Oxidation of various reactive dyes with in situ electro-generated active chlorine for textile dyeing industry wastewater treatment. *J Hazard Mater*, *136*(2), 203–212. https://doi.org/10.1016/j.jhazmat.2005.11.096
34. Raju, G. B., Karuppiah, M. T., Latha, S. S., Parvathy, S., Prabhakar, S. (2008). Treatment of wastewater from synthetic textile industry by electrocoagulation–electro-oxidation. *Chemical Engineering Journal*, *144*(1), 51–58. https://doi.org/10.1016/j.cej.2008.01.008
35. Ridruejo, C., Salazar, C., Cabot, P. L., Centellas, F., Brillas, E., Sirés, I. (2017). Electrochemical oxidation of anaesthetic tetracaine in aqueous medium: Influence of the anode and matrix composition. *Chemical Engineering Journal, 326*, 811–819. https://doi.org/10.1016/j.cej.2017.04.139
36. Robinson, T., McMullan, G., Marchant, R., Nigam, P. (2001). Remediation of dyes in textile effluent: a critical review on current treatment technologies with a proposed alternative. *Bioresource Technology*, *77*(3), 247–255. https://doi.org/10.1016/S0960-8524(00)00080-8
37. Sakalis, A., Mpoulmpasakos, K., Nickel, U., Fytianos, K, Voulgaropoulos, A. (2005). Evaluation of a novel electrochemical pilot plant process for azo dyes removal from textile wastewater. *Chemical Engineering Journal*, *111*(1), 63–7. https://doi.org/10.1016/j.cej.2005.05.008
38. Sandhya, S. (2010). Biodegradation of azo dyes under anaerobic condition: Role of azoreductase. In H. A. Erkurt (Ed.), *Biodegradation of azo dyes. The handbook of environmental chemistry* (vol.9) (pp.39-57). Berlin, Heidelberg: Springer. https://doi.

org/10.1007/698_2009_43

39. Saritha, V., Srinivas, N., Srikanth Vuppala, N.V. Analysis and optimization of coagulation and flocculation process. *Appl Water Sci 7*, 451–460 (2017). https://doi.org/10.1007/s13201-014-0262-y
40. Semeraro, P., Rizzi, V., Fini, P., Matera, S., Cosma, P., Franco, E., Rocío García c, Marcela Ferrandiz, Estrella Núne, Jose Antonio Gabaldon, Isabel Fortea, Enrique Perez, Miguel Ferrandiz. 2015. Interaction between industrial textile dyes and cyclodextrins. *Dyes and Pigments*, *119*(2015), 84–94. https://doi.org/10.1016/j.dyepig.2015.03.012
41. Sharma, S. K. (2011). *Green chemistry for environmental remediation*. Springer. https://doi.org/10.1007/978-1-4419-8071-1
42. Solís, M., Solís, A., Pérez, H. I., Manjarrez, N., Flores, M. (2012). Microbial decolouration of azo dyes: A review. *Process Biochemistry*, *47*(11), 1723–1748. https://doi.org/10.1016/j.procbio.2012.08.014
43. Spagni, A., Grilli, S., Casu, S., Mattioli, D., (2010). Treatment of a simulated textile wastewater containing the azo dye reactive orange 16 in an anaerobic-biofilm anoxic–aerobic membrane bioreactor. *Int. Biodeter. Biodegr*. *64*, 676–681. https://doi.org/10.1016/j.ibiod.2010.08.004
44. Szpyrkowicz, L., Juzzolino, C., Kaul, S. N. 2001 A Comparative study on oxidation of disperse dyes by electrochemical process, ozone, hypochlorite and Fenton reagent. *Water Res*, *35*(9), 2129–2136. https://doi.org/10.1016/S0043-1354(00)00487-5
45. Torrades, F., García-Hortal, J. A., García-Montaño, J. (2015). Mineralization of hetero bi-functional reactive dye in aqueous solution by Fenton and photo-Fenton reactions. *Environmental Technology*, *36*(16), 2035–2042. https://doi.org/10.1080/09593330.2015.1019931
46. Wang, S., Huang, Y., Meng, X., Liu, X. (2020). Highly efficient and heterogeneous OMS-2 for the direct oxidative degradation of organic dyes under acidic conditions. Inorganic Chemistry *Communications*, *117*(2020), 107969. https://doi.org/10.1016/j.inoche.2020.107969
47. Wong, P. W., Teng, T. T., Nik Norulaini, N. (2007). Efficiency of the coagulation-flocculation method for the treatment of dye mixtures containing disperse and reactive dye. *Water Quality Research Journal of Canada*, *42*(1), 54–62. https://doi.org/10.2166/wqrj.2007.008
48. Verma, A.K., Dash, R.R., Bhunia, P. (2012). A review on chemical coagulation/flocculation technologies for the removal of colour from textile wastewaters. *J. Environ. Manag*, *93*, 154e168. https://doi.org/10.1016/j.jenvman.2011.09.012
49. Zhou, X., Zhou, Y., Liu, J., Song, S., Sun, J., Zhu, G., Gong H., Wang, L., Wu, C., Li, M. (2019). Study on the pollution characteristics and emission factors of PCDD/Fs from disperse dye production in China, *Chemosphere*, *228*, 328–334. https://doi.org/10.1016/j.chemosphere.2019.04.136
50. Yilmaz, A. E., Boncukcuoğlu, R., Kocakerim, M. M. (2007). A quantitative comparison between electrocoagulation and chemical coagulation for boron removal from boron-containing solution. *J Hazard Mater*, *149*(2), 475–481. https://doi.org/10.1016/j.jhazmat.2007.04.018